Downregulation of *miR-486-5p* contributes to tumor progression and metastasis by targeting protumorigenic *ARHGAP5* in lung cancer

J Wang[1,7], **X Tian**[1,7], **R Han**[1], **X Zhang**[2], **X Wang**[3], **H Shen**[1], **L Xue**[1], **Y Liu**[3], **X Yan**[1], **J Shen**[4], **K Mannoor**[4], **J Deepak**[5], **JM Donahue**[6], **SA Stass**[4], **L Xing**[1], and **F Jiang**[4]

[1]Department of Pathology, Hebei Medical University, Shijiazhuang, China

[2]Department of Pathology, Second Hospital of Hebei Medical University, Shijiazhuang, China

[3]Department of Pathology, Tumor Hospital of Hebei Medical University, Shijiazhuang, China

[4]Department of Pathology, University of Maryland School of Medicine, Baltimore, MD, USA

[5]Department of Medicine, University of Maryland School of Medicine, Baltimore, MD, USA

[6]Department of Surgery, University of Maryland School of Medicine, Baltimore, MD, USA

Abstract

We have previously shown that *miR-486-5p* is one of the most downregulated micro RNAs in lung cancer. The objective of the study was to investigate the role of *miR-486-5p* in the progression and metastasis of non-small-cell lung cancer (NSCLC). We evaluated *miR-486-5p* expression status on 76 frozen and 33 formalin-fixed paraffin-embedded tissues of NSCLC by quantitative reverse transcriptase PCR to determine its clinicopathologic significance. We then performed function analysis of *miR-486-5p* to determine its potential roles on cancer cell migration and invasion *in vitro* and metastasis *in vivo*. We also investigated the target genes of *miR-486-5p* in lung tumorigenesis. *miR-486-5p* expression level was significantly lower in lung tumors compared with their corresponding normal tissues ($P<0.0001$), and associated with stage ($P =0.0001$) and lymph node metastasis of NSCLC ($P = 0.0019$). Forced expression of *miR-486-5p* inhibited NSCLC cell migration and invasion *in vitro* and metastasis in mice by inhibiting cell proliferation. Furthermore, ectopic expression of *miR-486-5p* in cancer cells reduced *ARHGAP5* expression level, whereas *miR-486-5p* silencing increased its expression. Luciferase assay demonstrated that *miR-486-5p* could directly bind to the 3′-untranslated region of *ARHGAP5*. The expression level of *miR-486-5p* was inversely correlated with that of *ARHGAP5* in lung tumor tissues ($P =0.0156$). Reduced expression of *ARHGAP5* considerably inhibited lung cancer cell migration and invasion, resembling that of *miR-486-5p* overexpression. *miR-486-5p* may act as a tumor-suppressor contributing to the progression and metastasis of NSCLC by targeting *ARHGAP5*. *miR-486-5p* would provide potential diagnostic and therapeutic targets for the disease.

Correspondence: Dr L Xing, Department of Pathology, Hebei Medical University, No. 361 East Zhongshan Road, Shijiazhuang 050017, China or Dr F Jiang, Department of Pathology, University of Maryland School of Medicine, 10 South Pine Street, MSTF 7th floor, Baltimore, MD 21201-1192, USA. xinglingxiao@hotmail.com or fjiang@som.umaryland.edu.
[7]These authors contributed equally to this work.

CONFLICT OF INTEREST
The authors declare no conflict of interest.

Keywords

miR-486-5p; tumor-suppressor gene; lung cancer; *ARHGAP5*; therapy

INTRODUCTION

Lung cancer is the leading cause of cancer-related death worldwide, mainly because it is often diagnosed at advanced stage accompanied by extensive invasion and metastasis.[1] Non-small-cell lung cancer (NSCLC) accounts for at least 80% of lung cancers.[1] Therefore, investigations of the molecular mechanisms underlying progression and metastasis of NSCLC may help develop novel prognostic biomarkers and therapeutic targets for the malignancy, and thus are clinically important.

Micro RNAs (MiRNAs) are endogenous, ~22-nucleotide-long, non-coding RNAs.[2] Individual miRNAs can target multiple distinct transcripts, and hence control a wide range of biological processes.[3–5] Abnormal expressions of miRNAs have frequently been observed in various types of cancers.[6] Importantly, downregulations of some miRNAs can motivate tumorigenesis by regulating several key pathways, including promoting cellular proliferation, evading apoptosis, stimulating angiogenesis and invasion and metastasis.[7,8] Therefore, the miRNAs have functions of tumor suppressors in cancer development and progression.[7,9] Using microarray to analyze primary lung tumor tissues for miRNA expressions, we have identified a set of 26 miRNAs whose abnormal expressions are associated with NSCLC.[3,4] *miR-486-5p* is one of the most downregulated miRNAs in lung tumor tissues. We recently showed that analyzing expression levels of the miRNAs, particularly *miR-486-5p*, in sputum and plasma could provide a diagnostic approach for NSCLC.[3–5]

In the study, we aimed to evaluate the possible roles and related target genes of *miR-486-5p* in tumorigenesis of NSCLC. We found that the expression level of *miR-486-5p* was significantly lower in NSCLC tissues than in the corresponding normal lung tissues, and inversely associated with advanced stage and lymph node metastasis of NSCLC. Furthermore, enforced *miR-486-5p* expression restrained lung cancer cell migration and invasion *in vitro* and metastasis *in vivo*. In addition, *ARHGAP5*, a protumorigenic gene, was identified as a functional target of *miR-486-5p*. Therefore, *miR-486-5p* downregulation contributes to lung cancer progression and metastasis through regulating *ARHGAP5*.

RESULTS

Reduced expression of *miR-486-5p* is inversely associated with advanced stage and lymph node metastasis of NSCLC

We previously reported that *miR-486-5p* was underexpressed in NSCLC by using microarray analysis.[3–5] To determine the clinicopathologic significance of the *miR-486-5p* aberration, we evaluated the expression level of *miR-486-5p* in 76 pairs of frozen NSCLC tissues and the corresponding normal lung tissues using quantitative reverse transcriptase PCR (qRT–PCR). *MiR-486-5p* expression was not significantly associated with age and gender of the patients and histological types of NSCLC (Table 1). However, the expression level was remarkably lower in NSCLC tissues than in their matched normal tissues ($P < 0.0001$) (Figure 1a). Furthermore, the expression level of *miR-486-5p* in tumor tissues statistically decreased with increasing stage of NSCLC ($P < 0.0001$) (Figure 1b). In addition, *miR-486-5p* expression was significantly lower in NSCLC that displayed lymph node metastasis than in NSCLC that did not have ($P = 0.0019$) (Figure 1c). Moreover, the observations were confirmed in formalin-fixed paraffin-embedded (FFPE) specimens of 33

NSCLC tissues and the paired normal lung tissues (Supplementary Table 1). Therefore, the low *miR-486-5p* expression is closely related to the progression and metastasis of NSCLC.

Ectopic overexpression of *miR-486-5p* restrains cell proliferation, migration and invasion of NSCLC cells

As a low level of *miR-486-5p* expression in NSCLC is a common molecular incident and correlated with advanced stage and metastasis of the disease, we hypothesize that ectopic expression of *miR-486-5p* in NSCLC can exert inhibitory effects on cell growth and invasion. To validate the hypothesis, we transfected a *miR-486-5p* mimic or scrambled sequence into A549 and H157 NSCLC cells, which had low basal levels of *miR-486-5p* in NSCLC cell lines (Supplementary Figure 1). Successful overexpression of *miR-486-5p* in the cells was confirmed by qRT–PCR. Interestingly, methylthiazol tetrazolium assay showed that forced expression of *miR-486-5p* could impair growth rate of the NSCLC cells (Figures 2a and b).

To explore the possible mechanism of overexpression of *miR-486-5p* underlying the inhibitory effect on cell growth, we performed 5-bromo-2′-deoxyuridine (BrdU) incorporation assay and apoptotic analysis. BrdU incorporation level was statistically lower in cells transfected with *miR-486-5p* mimic than in cells with scrambled sequence ($P<0.05$) (Supplementary Figure 2), suggesting that ectopic expression of *miR-486-5p* could reduce the proliferation of NSCLC cells. Annexin V fluorescein isothiocyanate (V-FITC) apoptotic assay showed that there was no significant difference of apoptotic rate between cells with *miR-486-5p* mimic and control cells ($P>0.05$) (Supplementary Figure 3). Therefore, ectopic expression of *miR-486-5p* might reduce cell growth of NSCLC mainly through inhibiting cell proliferation. Furthermore, *miR-486-5p* overexpression could suppress the migratory and invasive abilities of the NSCLC cells (H157 and A549) determined by Transwell assay (Figures 2c and d). Taken together, *miR-486-5p* might have tumor-suppressor function.

Overexpression of *miR-486-5p* inhibits NSCLC metastasis *in vivo*

To further investigate the role of *miR-486-5p* in tumorigenesis of NSCLC cells, we injected mice through tail vein with H460-bioluminescent cells that were transfected with *miR-486-5p* mimic or scrambled sequence control. The mice were monitored for tumor formation and metastasis by bioluminescence imaging. Positive imaging was observed in the lungs of the mice injected with H460 cells with scrambled sequence after 1 week (Figure 3a). Furthermore, additional positive signals outside lungs could be found in neck and abdomen of the mice in week 7 (Figure 3a). However, although positive signals were noticed in the lungs of the mice injected with H460 cells with *miR-486-5p* mimic in week 1, no positive imaging besides the lungs was found in week 7 (Figure 3b). We used mean photon counts of bioluminescence to evaluate malignant lesions in the mice as previously described.[10] Mean photon counts of malignant nodules in the lungs of all mice inoculated with H460 cells with scrambled sequence was markedly higher than that seen in all mice injected with H460 cells with *miR-486-5p* mimic ($P<0.05$) (Supplementary Figure 4). In addition, mean photon counts of metastatic lesions was significantly higher in mice injected with H460 cells with scrambled sequence compared with mice injected with H460 cells with *miR-486-5p* mimic ($P<0.05$) (Supplementary Figure 5). Moreover, the average weight of primary lung tumors derived from H460 cells with scrambled sequence was significantly larger than that from H460 cells with *miR-486-5p* mimic ($P = 0.008$) (Supplementary Figure 6). Primary tumors in lungs generated from H460 cells transfected with scrambled sequence and the associated metastatic tumors in lymph nodes were confirmed by hematoxylin and eosin staining on tissue sections (Figures 3c and d). Therefore, *miR-486-5p* overexpression could inhibit lung tumorigenicity and metastasis *in vivo*.

Furthermore, we performed immunohistochemical analysis of Ki-67, a marker of proliferation, on tissue sections of tumors excised from mice. The number of Ki-67-positive cells was statistically lower in tumors created from cancer cells with *miR-486-5p* mimic than in tumors generated from cancer cells with scrambled sequence (Supplementary Figure 7A) (*P* =0.009). Moreover, we carried out the terminal nucleotidyl transferase-mediated nick end labeling assay for evaluating apoptosis.

Percentage of apoptotic cells was not statistically different between tumors created from cells with miR-486-5p mimic and those generated from cancer cells with scrambled sequence (Supplementary Figure 7B) (*P* =0.65). Therefore, the inhibition of *in vivo* tumorigenicity by forced *miR-486-5p* expression is likely attributed to decreased cell proliferation.

Protumorigenic factor *ARHGAP5* is a direct target of *miR-486-5p*

To elucidate the mechanisms responsible for the tumor-suppressive abilities of *miR-486-5p*, we used bioinformatics analysis to identify its target genes. *ARHGAP5* was identified as one of the candidate targets of *miR-486-5p* (Supplementary Table 2). *MiR-486-5p* can potentially bind to the 3′-untranslated region (UTR) of *ARHGAP5* (Figure 4a). Previous studies showed that *ARHGAP5* could inhibit RhoA activity and contribute to spreading and migration by enhancing cell protrusion, elongation and polarity.[3–5] Furthermore, *ARHGAP5* displayed a high expression level in aggressive tumors and had protumorigenic function in carcinogenesis.[11,12] Therefore, we paid special attention to *ARHGAP5* for deep investigation in the present study.

To determine whether *ARHGAP5* could be regulated by *miR-486-5p*, we performed luciferase reporter assay. The luciferase activity of *ARHGAP5*-3′-UTR was reduced by ~60% in cells expressing *miR-486-5p* compared with those expressing the control (Figure 4b). We further transfected the cells with *miR-486-5p* mimic to produce overexpression of *miR-486-5p* in cancer cells and then measured *ARHGAP5* expressions by using western blotting with p190-B antibody. Forced expression of *miR-486-5p* produced a decrease of *ARHGAP5* expression (Figures 4c and d). Therefore, it is likely that *miR-486-5p* may bind to the 3′-UTR sequences of *ARHGAP5*, and might inhibit its expression through post-transcriptional regulation.

ARHGAP5 is involved in *miR-486-5p*-induced suppression of NSCLC cell proliferation, migration and invasion

To further explore the functions of *ARHGAP5* in lung tumorigenesis, we used specific small interfering RNAs against *ARHGAP5* (si-*ARHGAP5*) to reduce expression of *ARHGAP5* in NSCLC cells. As shown in Figure 5a, si-*ARHGAP5* dramatically reduced *ARHGAP5* expression. Methylthiazol tetrazolium and colony formation assays showed that cell growth and proliferation were significantly repressed becauae of downregulation of *ARHGAP5* (Figure 5b). Furthermore, Wound healing and Transwell assays indicated that *ARHGAP5* downregulation inhibited NSCLC cell migration and invasion (Figures 5c and d), which, resembled the inhibitory effects of *miR-486-5p* on the cancer cells. Therefore, *ARHGAP5* might be protumorigenic factor in the development and progression of NSCLC.

To determine whether deregulation of *ARHGAP5* by *miR-486-5p* involved in cell migration and invasion, we transfected NSCLC cells with *miR-486-5p* inhibitor and si-*ARHGAP5*. Compared with control cell group, the cells transfected with *miR-486-5p* inhibitor displayed higher expression of *ARHGAP5*, whereas the cells with the cotransfection of both *miR-486-5p* inhibitor and si-*ARHGAP5* exhibited lower *ARHGAP5* expression (Figures 6a and b). Interestingly, the cells transfected with *miR-486-5p* inhibitor displayed higher

migration- and invasion potential compared with the cells transfected with both *miR-486-5p* inhibitor and si-*ARHGAP5* (Figures 6c and d). The observations suggest that the effects of *miR-486-5p* downregulation on the promotion of cancer cell migration and invasion could be diminished by si-*ARHGAP5*. Therefore, *ARHGAP5* may have an important role in the cell migration and invasion of NSCLC mediated by *miR-486-5p*.

Upregulation of *ARHGAP5* is inversely associated with downregulation of *miR-486-5p* in clinical specimens of NSCLC

To further investigate clinical significance of *ARHGAP5* expression, we examined *ARHGAP5* expression by using immunohistochemical analysis on FFPEs of 54 NSCLC with p190-B antibody. As shown in Figure 7a, p190-B exhibited negative or weak staining in alveolar epithelial cells and bronchial epithelial cells of normal lung tissue. In contrast, p190-B displayed positive staining in tumor tissues with different intensity (Figures 7b and c). Furthermore, p190-B expression was positively correlated with tumor, nodes and metastasis-classification (TNM) stage and lymph node metastasis of NSCLC (All *P*<0.001) (Supplementary Table 3). Taken together, *ARHGAP5* is frequently overexpressed in NSCLC and the elevated expression is positively associated with the progression of the disease.

To explore the relationship between *miR-486-5p* and *ARHGAP5* in clinical specimens, we compared *ARHGAP5* expression data from immunohistochemistry analysis with results of *miR-486* expression level from qRT–PCR analysis on FFPE specimens of 33 NSCLC tissues. There was an inverse correlation between *miR-486-5p* and *ARHGAP5* expressions in the specimens (*P* =0.0156) (Figure 7d). Therefore, the findings further signify that *ARHGAP5* upregulation might result from suppression of *miR-486-5p* in NSCLC.

DISCUSSION

Reduced *miR-486-5p* expression is a frequent molecular event in human malignances.[5,13–15] We have showed that *miR-486-5p* is repressed in early-stage NSCLC by using microarray analysis.[3–5] We further demonstrated that analyzing expression of *miR-486-5p* in sputum and plasma specimens could provide a diagnostic approach for the early detection of lung cancer.[3–5] Oh *et al.*[16] recently found that *miR-486-5p* might target *OLFM4* anti-apoptotic factor, and hence had important function in the progression and metastasis of gastric cancer. However, the exact mechanism of *miR-486-5p* dysregulation in NSCLC remains unknown. In the present study, we first found that *miR-486-5p* was frequently downregulated in lung tumor tissues and the reduced *miR-486-5p* expression was closely related to advanced stage and lymph node metastasis of NSCLC. Furthermore, we demonstrated that *miR-486-5p* overexpression could suppress NSCLC cell proliferation, migration and invasion *in vitro* and metastasis *in vivo*. In addition, we identified protumorigenic *ARHGAP5* as a target of *miR-486-5p*. Therefore, *miR-486-5p* could be a novel tumor-suppressor miRNA, and its downregulation might contribute to lung cancer progression and metastasis through regulating *ARHGAP5* function.

Elucidating the molecular mechanism(s) of lymph node metastasis is a critical issue, as lymph node metastasis is a fundamental factor in the determination of the clinical staging and prognosis of NSCLC. It is widely accepted that cellular adhesion, motility and invasion are required for the spreading of tumor cells from their primary tumor to lymph nodes in the process of metastasis. Interestingly, *ARHGAP5*-encoded protein is an important regulator of RhoA,[17,18] which is a prototypical member of the Rho GTPase family. Rho GTPase can regulate many cellular processes, particularly including cellular adhesion, motility and polarity.[18–23] Furthermore, upregulation of *ARHGAP5* in cancers can contribute to invasive and metastatic behavior. For example, *ARHGAP5* upregulation has protumorigenic functions

that enhance tumor cell migration in a variety of cancers, such as breast tumor,[24–26] hepatocellular carcinoma and melanoma.[16,27] In consistent with the previous findings, the results obtained from our current study demonstrated that *ARHGAP5* expression was significantly increased in NSCLC tissues, and the high expression level was correlated with a more aggressive behavior of the disease. Moreover, reduced *ARHGAP5* expression restrains cell growth, proliferation, migration and invasion of NSCLC. Therefore, upregulation of *ARHGAP5* has a vital tumorigenic role in carcinogenesis of NSCLC. In addition, our functional analysis showed that overexpression of *miR-486-5p* inhibited *ARHGAP5* expression and conferred inhibition of cell proliferation and migration, which was parallel to small interfering RNA-mediated knockdown of *ARHGAP5*. The observations would bring a new insight about the essential mechanisms of regulating the RhoA pathway in the progression and metastasis of NSCLC. Importantly, these findings reveal that *ARHGAP5* is a biologically significant target gene of *miR-486-5p*. Furthermore, the *miR-486-5p/ARHGAP5* pathway might be a previously unrecognized regulator involved in lung tumor progression and lymph node metastasis of NSCLC. Therefore, *miR-486-5p* may serve as a potential target for therapeutic intervention against invasive and metastatic NSCLC.

There are several possible reasons for the observation of downregulation of *miR-486-5p* in tumor tissues. For instance, *miR-486-5p* is located on chromosome 8p11.21, one of the most frequent genomic deletion regions that contain potential tumor-suppressor genes in various types of tumors, such as NSCLC.[17,18] Allelic loss of the genomic region may be responsible for the downregulation of *miR-486-5p*. Furthermore, *miR-486-5p* is located in a CpG island on chromosome 2q35. Epigenetic silencing through DNA methylation and/or histone deacetylation may also lead to *miR-486-5p* downregulation. Nevertheless, further studies are required to evaluate causes of *miR-486-5p* dysgulation in carcinogenesis of NSCLC.

ARHGAP5 is identified as a target of *miR-486-5p*. However, the antioncogenic properties of *miR-486-5p* downregulation might not solely be explained by its ability to regulate the single gene alone, because a single miRNA could regulate numerous genes in tumorigenesis.[19] Indeed, using bioinformatic prediction analysis, we identified at least eight other potential targets of *miR-486-5p*, including some cancer-related genes. For example, *OLFM4* was recently proposed as a biologically relevant *miR-486-5p* target in the context of gastric cancer.[16] Furthermore, *miR-486-5p* has been shown to target *PTEN* in muscle cells.[20] *PTEN* is a major negative regulator of the PI3-kinase pathway, which regulates growth, survival and proliferation.[21] *PTEN* has been identified as a tumor-suppressor that is mutated in a large number of cancers, including NSCLC.[22,23] Therefore, we cannot exclude the possibility that these candidate targets for *miR-486-5p* other than *ARHGAP5* could be involved in tumor-suppressive function of *miR-486-5p*. We are exploring the correlation between *miR-486-5p* and other target candidates and determining whether *miR-486-5p* can biologically regulate the potential targets in a different study. On the other hand, bioinformatic analysis suggests that the *ARHGAP5* may be targeted by more than 10 different miRNAs (Supplementary Table 4), implying that other miRNAs may also act to mediate function of *ARHGAP5* in lung tumorigenesis. For example, *miR-15a* is one of the miRNAs that are predicted as candidates to regulate *ARHGAP5*. Interestingly, *miR-15a* has previously been identified as a tumor-suppressor in chronic lymphocytic leukemia, multiple myeloma and acute myeloid leukemia by regulating cell proliferation.[28] Therefore, future studies to identify additional novel targets of *miR-486-5p* and other miRNAs that can also regulate *ARHGAP5* will allow us to have deep understanding mechanisms underlying the development and progression of NSCLC.

In conclusion, reduced *miR-486-5p* expression frequently exists in lung tumor, and is closely associated with progression and metastasis of NSCLC. *MiR-486* could act as a tumor-

suppressor in the development and progression of NSCLC through targeting *ARHGAP5*. With more understanding its function, *miR-486-5p* may be used as a potential metastatic/ prognostic marker and therapeutic target in treatment of NSCLC.

MATERIALS AND METHODS

Surgical tissue specimens

The study protocol was approved by the Institutional Review Boards of Tumor Hospital of Hebei Medical University and University of Maryland School of Medicine. The frozen surgical tumor and corresponding normal lung tissues of 76 patients with NSCLC were obtained. Demographic and clinical characteristics of the patients are shown in Table 1. The 76 NSCLC patients consist of 20 females and 56 males, ages 54–83 years (median, 69 years). Thirty-nine patients were diagnosed with adenocarcinoma and 37 with squamous cell carcinoma. Nineteen patients had stage I disease, 33 patients had stage II disease, and 24 patients had stage III disease. Furthermore, FFPE sections of lung tumor and corresponding normal lung tissues of 54 NSCLC patients were also collected (Supplementary Table 3). All variants, including age, sex, stage and lymph node metastasis, were obtained from clinical and pathologic records. None of the patients had received preoperative adjuvant chemotherapy or radiotherapy.

Cell culture

Human NSCLC cell lines (H460, A549, H1944, H358, H157, H1792, H226, H292, and H522) were obtained from the American Type Culture Collection. Cells were maintained at 37 °C in a humidified air atmosphere containing 5% carbon dioxide in RPMI1640 (MGC-803, HGC-27), F12 (AGS) or Dulbecco's Modified Eagle's Media (HEK293T) supplemented with 10% fetal bovine serum.

RNA extraction and quantitative real-time PCR

Total RNA from cultured cells and frozen tissue specimens was extracted using a mirVana miRNA Isolation Kit (Ambion, Austin, TX, USA) according to the manufacturer's instructions. Total RNA from 4 μm-thick FFPE sections was isolated using a RecoverAll Total Nucleic Acid Isolation Kit (Ambion) optimized for FFPE samples according to the manufacturer's instructions. qRT–PCR assays were carried out to detect miRNA expression using Taqman miRNA assays (Applied Biosystems, Foster City, CA, USA) as described in our previous study.[3–5] *U6* small nuclear RNA was used as an internal control. Furthermore, *ARHGAP5* transcript expression was measured by using qRT–PCR with forward primer 5′-(CATCTGTTTTTGGCCAACCT)-3′ and reverse primer 5′-(GTGGAGGAGCCA CAATGTTT)-3′. To determine *ARHGAP5* transcript expression level, *β-Actin* was used as an internal control. Experiments were repeated at least three times.

Enforcing or reducing expressions of *miR-486-5p* in NSCLC cells

To force expression of *miR-486-5p* in cancer cells, cells were transfected with precursor molecules mimicking *miR-486-5p* (Ribobio Co., Guangzhou, China) or scrambled sequence by using LipoFectamine 2000 (Invitrogen, Grand Island, NY, USA) according to the manufacturer's instructions. To reduce expression of *miR-486-5p*, an inhibitor of *miR-486* or negative inhibitor control (Ambion) was transfected into cancer cells by using HiPerFect transfection reagent (Qiagen, Valencia, CA, USA) according to the manufacturer's instructions. Experiments were repeated at least three times.

Small interfering RNA silencing of *ARHGAP5*

Sequences of small interfering RNA specifically against *ARHGAP5* (si-*ARHGAP5*) are 5′-AGAUCAUAAUAUCAAUCUATT-3′. Transfections were performed using Lipofectamine 2000 reagent (Invitrogen) following the manufacturer's protocol with si-*ARHGAP5* (Genephma, Shanghai, China) or scrambled sequences. At least three independent experiments were carried out.

Bioinformatics

Two software programs, TargetScan 5.2 (Release 5.2, June 2011; http://www.targetscan.org/) and miRecords (http://mirecords.biolead.org/), were used to predict the potential target genes of *miR-486-5p*.

ARHGAP5 gene 3′-UTR luciferase reporter assay

To create 3′-UTR luciferase reporter construct of *ARHGAP5*, 1757-bp sequences from putative *miR-486-5p*-binding sites were synthesized and ligated into the pGL3-REPORT vector (Promega, Shanghai, China). The following primers were used to amplify the 3′-UTR of *ARHGAP5*: 5′-CCG ACGCGTATGCTTGTGGCTAAAGTGAGT-3′ and 5′-CCGCTCGAGAAACAGTGAAACCTTCCAGTAA-3′. The amplified fragment was cloned into pGL3 luciferase report vector at Mlu I and Xho I sites. The sequence of plasmid (pGL3-*ARHGAP5*) was confirmed by DNA sequencing. Cancer cells (5×10^4 per well) were seeded in a 24-well plate the day before transfection, and then co-transfected with firefly luciferase-3′-UTR (pGL$_3$-ARHGFAP5, 500 ng) and pRL-TK vector (Promega) along with *miR-486-5p* mimics or control (Ribobio Co.). After 2 days, firefly luciferase and Renilla luciferase were measured by using synergy HT microplate reader (Biotek, Beijing, China) with the Dual-Glo Luciferase assay system (Promega). Luciferase activities were normalized to Renilla luciferase activity. Experiments were repeated at least three times.

Methylthiazol tetrazolium assay

Methylthiazol tetrazolium assay was performed as previously described.[29,30] Briefly, after transfection, cells were plated in 96-well plates, and the cells viability was assessed in ten replicates. The experiments were done at least three times.

Colony formation assay

For colony formation assays, after 24-hour post-transfection, the cells were diluted and replated in six-well plates. After 10 days, visible colonies were fixed with methanol, stained with crystal violet, counted and normalized to the control group. The experiments were performed at least three times.

BrdU incorporation assay

Cells were plated on coverslips. BrdU (10 μM) was added to the culture medium for 12 h. Cells were fixed in 4% paraformaldheyde for 10 min, washed with phosphate-buffered saline, and incubated with HCl 2 N for 2 min. Immunocytofluorescence was performed on cells with mouse anti BrdU antibody (Dako, Carpinteria, CA, USA), and the fluorochrome conjugated secondary antibody against mouse Ig (Invitrogen). DAPI was used to counterstain the nuclei. Immunostained cells were analyzed under fluorescent microscope (Leica, Solms, Germany). Results were expressed as the ratio of BrdU- to DAPI-positive cells. The experiments were performed at least three times.

Annexin V apoptosis assay

Cells were stained with annexin V fluorescein isothiocyanate (V-FITC) and propidium iodide (PI) using the Annexin V-FITC Kit (Beckman Colter, Boulevard Brea, CA, USA) for flow cytometric analysis. The apoptotic index was calculated as the percentage of annexin V +/PI-cells.

Wound-healing assay

To determine cell migration, cells were seeded in six-well plates and incubated to generate confluent cultures. Wounds were scratched in the cell monolayer using a 200 micropipette tip. The cells were rinsed with phosphate-buffered saline. The migration of the cells at the edge of the scratch was monitored at time 0, 24 and 48 h, respectively. The cells were stained and photographed. At least three independent experiments were carried out.

Transwell assay

To determine cell invasion and migration, after transfection, cells were plated in medium without serum in the top chamber of a transwell (Corning, Horseheads, NY, USA). The bottom chamber contained standard medium with 10% fetal bovine serum. After 24-h incubation, the cells that had migrated to the lower surface of the membrane were fixed with formalin, stained with crystal violet and photographed under microscope. Cell numbers were counted under a light microscope at $\times 400$ magnification. Experiments were carried out at least three times.

In vivo metastatic assay

H460-*luc2*, a luciferase expressing NSCLC cell line stably transfected with firefly luciferase gene (*luc2*) was obtained from Caliper Life Sciences, Inc. (Hopkinton, MA, USA). 5×10^6 H460-*luc2* cells transfected with *miR-486-5p* mimic or scrambled sequence using LipoFectamine 2000 (Invitrogen). The cancer cells were injected via the tail vein into ten athymic Swiss mice per group, respectively. D-Luciferin (Xenogen Co., Alameda, CA, USA) was injected into animals at a dosage of 150 mg/kg body weight for luciferin *in vivo* imaging by using IVIS 200 Imaging System (Xenogen Corp.) as described in our previous work.[30] We monitored *in vivo* tumor formation by bioluminescence imaging in 1, 2, 3, 4, 5, 6 and 7 weeks after injection of the H460-*luc2* cells, because bioluminescence is a sensitive and cost-effective approach to quantify *in vivo* tumors that are not grossly measurable.[10] Furthermore, we used mean photon counts of bioluminescence to evaluate malignant lesions in ten mice per group as previously described.[10,30] In addition, mice were killed at 8 weeks for full autopsy. All tumors were excised, weighed, harvested, fixed and embedded. The average weight of tumors was calculated and compared between the groups. Tissue specimens were also stained by hematoxylin and eosin for histological study.

Western blot

Total proteins (100 μg) extracted from cell lines and tissues were analyzed by SDS–polyacrylamide gel electrophoresis and were transferred electrophoretically to nitrocellulose membrane. To evaluate expression of *ARHGAP*, blots were blocked with 5% non-fat milk in Tris-Buffered Saline and Tween 20, and incubated with a primary rabbit monoclonal antibody, p190-B (Epitomics, Inc., Hangzhou, China). The monoclonal p190-B antibody was produced by immunizing animals with a synthetic peptide corresponding to residues in human p190-B RhoGAP. Furthermore, the specificity of the antibody for p190-B RhoGAP was confirmed by the company (Epitomics). In addition, the antibody produced a single clean band of 190 kDa in Western blot analysis of surgical human lung tissue specimens (Supplementary Figure 8). Antibody for β-actin (Santa Cruz Biotechnology, Santa Cruz,

CA, USA) was used as a control. The blots were then reprobed with secondary antibody and visualized by the ECL system (GE Healthcare Life Sciences, Piscataway, NJ, USA).

Immunohistochemistry assay

Immunohistochemistry staining for determining *ARHGAP5* expression on human lung tissue specimens was done on FFPEs using p190-B antibody (Epitomics). As a negative control, primary antibody was replaced by phosphate-buffered saline. All sections were examined and scored independently by two investigators without any knowledge of the clinicopathological data of the patients. At least five fields per slide were randomly chosen for analysis of immunohistochemistry staining. The immunohistochemistry staining was evaluated according to the intensity of reactivity using a four-tier system: 0, no staining (−); 1, weak staining (+); 2, moderate staining (+ +); and 3, strong staining (+ + +).

To assess cell proliferation status on tissue sections of tumors excised from mice, the mouse-anti-human Ki-67 monoclonal antibody (Dako, Glostrup, Denmark) was applied to determine nuclear expression of Ki-67 as described in our previous report.[31]

In situ detection of apoptosis by terminal nucleotidyl transferase-mediated nick end labeling assay

In situ terminal nucleotidyl transferase-mediated nick end labeling assay was carried out on 4-μm thick sections of tumor specimens from mice for evidence of the damaged DNA characteristic of apoptotic cells as previously described.[32] Cells for apoptosis were identified as dark brown nuclei under a microscope. The number of apoptotic cells was counted from a minimum of five fields with >1000 cells/field.

Statistical analysis

The differences of *in vitro* results between groups were analyzed by using Student *t*-test when there were only two groups, or evaluated by one-way analysis of variance when there were more than two groups. We used mean photon counts of bioluminescence to evaluate malignant lesions in all 10 mice per group as previously described.[29,30] To evaluate differences of tumor metastasis of mice between two groups, statistical significance of differences of photon counts was assessed by two-sided Student's *t*-tests. Difference of *miR-486-5p* expressions between tumor tissues and normal lung tissues of human subjects was calculated by a two-tailed independent samples *t*-test. Spearman's correlation analysis was used to determine associations between *miR-486-5p* expression and clinical characteristics of the NSCLC patients, and correlation between *miR-486-5p* and *ARHGAP5* expressions. In all cases, a *P*-value <0.05 was considered statistically significant.

Supplementary Material

Refer to Web version on PubMed Central for supplementary material.

Acknowledgments

References

1. Tarver T. Cancer facts & figures 2012. American Cancer Society (ACS). J Consumer Health Internet. 2012; 16:366–367.

2. Ambros V. MicroRNA pathways in flies and worms: growth, death, fat, stress, and timing. Cell. 2003; 113:673–676. [PubMed: 12809598]

3. Yu L, Todd NW, Xing L, Xie Y, Zhang H, Liu Z, et al. Early detection of lung adenocarcinoma in sputum by a panel of microRNA markers. Int J Cancer. 2010; 127:2870–2878. [PubMed: 21351266]

4. Xing L, Todd NW, Yu L, Fang H, Jiang F. Early detection of squamous cell lung cancer in sputum by a panel of microRNA markers. Mod Pathol. 2010; 23:1157–1164. [PubMed: 20526284]

5. Shen J, Liu Z, Todd NW, Zhang H, Liao J, Yu L, et al. Diagnosis of lung cancer in individuals with solitary pulmonary nodules by plasma microRNA biomarkers. BMC Cancer. 2011; 11:374. [PubMed: 21864403]

6. Xiao C, Rajewsky K. MicroRNA control in the immune system: basic principles. Cell. 2009; 136:26–36. [PubMed: 19135886]

7. Saito Y, Jones PA. Epigenetic activation of tumor suppressor microRNAs in human cancer cells. Cell Cycle. 2006; 5:2220–2222. [PubMed: 17012846]

8. Lu J, Getz G, Miska EA, Alvarez-Saavedra E, Lamb J, Peck D, et al. MicroRNA expression profiles classify human cancers. Nature. 2005; 435:834–838. [PubMed: 15944708]

9. Kent OA, Mendell JT. A small piece in the cancer puzzle: microRNAs as tumor suppressors and oncogenes. Oncogene. 2006; 25:6188–6196. [PubMed: 17028598]

10. Jenkins DE, Oei Y, Hornig YS, Yu SF, Dusich J, Purchio T, et al. Bioluminescent imaging (BLI) to improve and refine traditional murine models of tumor growth and metastasis. Clin Exp Metastasis. 2003; 20:733–744. [PubMed: 14713107]

11. Chakravarty G, Hadsell D, Buitrago W, Settleman J, Rosen JM. p190-B RhoGAP regulates mammary ductal morphogenesis. Mol Endocrinol. 2003; 17:1054–1065. [PubMed: 12637587]

12. Gen Y, Yasui K, Zen K, Nakajima T, Tsuji K, Endo M, et al. A novel amplification target, ARHGAP5, promotes cell spreading and migration by negatively regulating RhoA in Huh-7 hepatocellular carcinoma cells. Cancer Lett. 2009; 275:27–34. [PubMed: 18996642]

13. Tan X, Qin W, Zhang L, Hang J, Li B, Zhang C, et al. A 5-microRNA signature for lung squamous cell carcinoma diagnosis and hsa-miR-31 for prognosis. Clin Cancer Res. 2011; 17:6802–6811. [PubMed: 21890451]

14. Bansal A, Lee IH, Hong X, Anand V, Mathur SC, Gaddam S, et al. Feasibility of mcroRNAs as biomarkers for Barrett's Esophagus progression: a pilot cross-sectional, phase 2 biomarker study. Am J Gastroenterol. 2011; 106:1055–1063. [PubMed: 21407181]

15. Ragusa M, Majorana A, Statello L, Maugeri M, Salito L, Barbagallo D, et al. Specific alterations of microRNA transcriptome and global network structure in colorectal carcinoma after cetuximab treatment. Mol Cancer Ther. 2010; 9:3396–3409. [PubMed: 20881268]

16. Oh HK, Tan AL, Das K, Ooi CH, Deng NT, Tan IB, et al. Genomic loss of miR-486 regulates tumor progression and the OLFM4 antiapoptotic factor in gastric cancer. Clin Cancer Res. 2011; 17:2657–2667. [PubMed: 21415212]

17. Midorikawa Y, Yamamoto S, Tsuji S, Kamimura N, Ishikawa S, Igarashi H, et al. Allelic imbalances and homozygous deletion on 8p23. 2 for stepwise progression of hepatocarcinogenesis. Hepatology. 2009; 49:513–522. [PubMed: 19105209]

18. Jiang F, Yin Z, Caraway NP, Li R, Katz RL. Genomic profiles in stage I primary non small cell lung cancer using comparative genomic hybridization analysis of cDNA microarrays. Neoplasia. 2004; 6:623–635. [PubMed: 15548372]

19. Lim LP, Lau NC, Garrett-Engele P, Grimson A, Schelter JM, Castle J, et al. Microarray analysis shows that some microRNAs downregulate large numbers of target mRNAs. Nature. 2005; 433:769–773. [PubMed: 15685193]

20. Small EM, O'Rourke JR, Moresi V, Sutherland LB, McAnally J, Gerard RD, et al. Regulation of PI3-kinase/Akt signaling by muscle-enriched microRNA-486. Proc Natl Acad Sci USA. 2010; 107:4218–4223. [PubMed: 20142475]

21. Lee JO, Yang H, Georgescu MM, Di Cristofano A, Maehama T, Shi Y, et al. Crystal structure of the PTEN tumor suppressor: implications for its phosphoinositide phosphatase activity and membrane association. Cell. 1999; 99:323–334. [PubMed: 10555148]

22. Teng DH, Hu R, Lin H, Davis T, Iliev D, Frye C, et al. MMAC1/PTEN mutations in primary tumor specimens and tumor cell lines. Cancer Res. 1997; 57:5221–5225. [PubMed: 9393738]

23. Steck PA, Pershouse MA, Jasser SA, Yung WK, Lin H, Ligon AH, et al. Identification of a candidate tumour suppressor gene, MMAC1, at chromosome 10q23. 3 that is mutated in multiple advanced cancers. Nat Genet. 1997; 15:356–362. [PubMed: 9090379]

24. Heckman-Stoddard BM, Vargo-Gogola T, McHenry PR, Jiang V, Herrick MP, Hilsenbeck SG, et al. Haploinsufficiency for p190B RhoGAP inhibits MMTV-Neu tumor progression. Breast Cancer Res. 2009; 11:R61. [PubMed: 19703301]

25. Sordella R, Classon M, Hu KQ, Matheson SF, Brouns MR, Fine B, et al. Modulation of CREB activity by the Rho GTPase regulates cell and organism size during mouse embryonic development. Dev Cell. 2002; 2:553–565. [PubMed: 12015964]

26. McHenry PR, Sears JC, Herrick MP, Chang P, Heckman-Stoddard BM, Rybarczyk M, et al. P190B RhoGAP has pro-tumorigenic functions during MMTV-Neu mammary tumorigenesis and metastasis. Breast Cancer Res. 2010; 12:R73. [PubMed: 20860838]

27. Nakahara H, Mueller SC, Nomizu M, Yamada Y, Yeh Y, Chen WT. Activation of beta1 integrin signaling stimulates tyrosine phosphorylation of p190RhoGAP and membrane-protrusive activities at invadopodia. J Biol Chem. 1998; 273:9–12. [PubMed: 9417037]

28. Gao SM, Xing CY, Chen CQ, Lin SS, Dong PH, Yu FJ. miR-15a and miR-16-1 inhibit the proliferation of leukemic cells by down-regulating WT1 protein level. J Exp Clin Cancer Res. 2011; 30:110. [PubMed: 22133358]

29. Fan T, Li R, Todd NW, Qiu Q, Fang HB, Wang H, et al. Up-regulation of 14-3-3zeta in lung cancer and its implication as prognostic and therapeutic target. Cancer Res. 2007; 67:7901–7906. [PubMed: 17699796]

30. Mei YP, Liao JP, Shen J, Yu L, Liu BL, Liu L, et al. Small nucleolar RNA 42 acts as an oncogene in lung tumorigenesis. Oncogene. 2012; 31:2794–2804. [PubMed: 21986946]

31. Wang H, Zhang Z, Li R, Ang KK, Zhang H, Caraway NP, et al. Overexpression of S100A2 protein as a prognostic marker for patients with stage I non small cell lung cancer. Int J Cancer. 2005; 116:285–290. [PubMed: 15800916]

32. Gavrieli Y, Sherman Y, Ben-Sasson SA. Identification of programmed cell death in situ via specific labeling of nuclear DNA fragmentation. J Cell Biol. 1992; 119:493–501. [PubMed: 1400587]
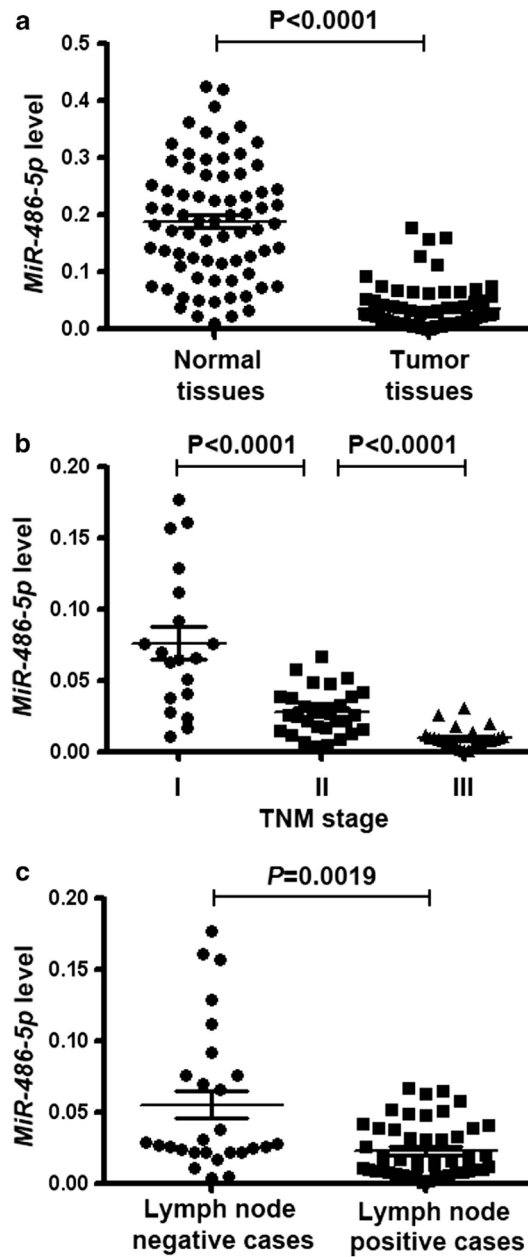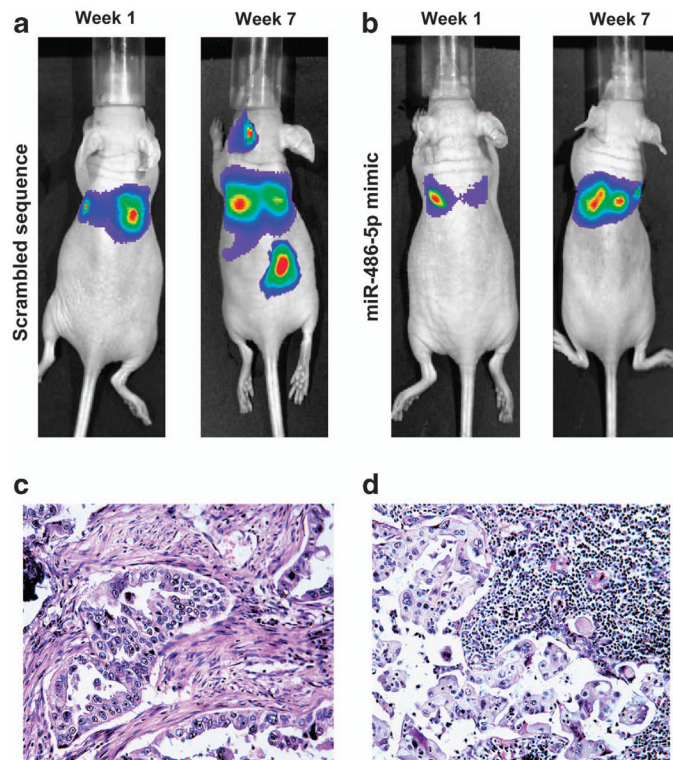
Figure 1.
Expression level of *miR-486-5p* is lower in lung tumor tissues than in the matched normal lung tissues and the reduced expression is associated with advanced clinical stage and lymph node metastasis of NSCLC. (**a**) *miR-486-5p* expression level was considerably lower in NSCLC tissues than in their matched normal tissues. The expression level of *miR-486-5p* was assessed in 76 pairs of primary NSCLC frozen tissues and the corresponding normal lung tissues using qRT–PCR. *U6* small nuclear RNA was used as an internal control. (**b**) Low-level expression of *miR-486-5p* was associated with high tumor stage of NSCLC (*P*<0.001). (**c**) Low-level expression of *miR-486-5p* was related with lymph node metastasis of NSCLC (*P* =0.0019).
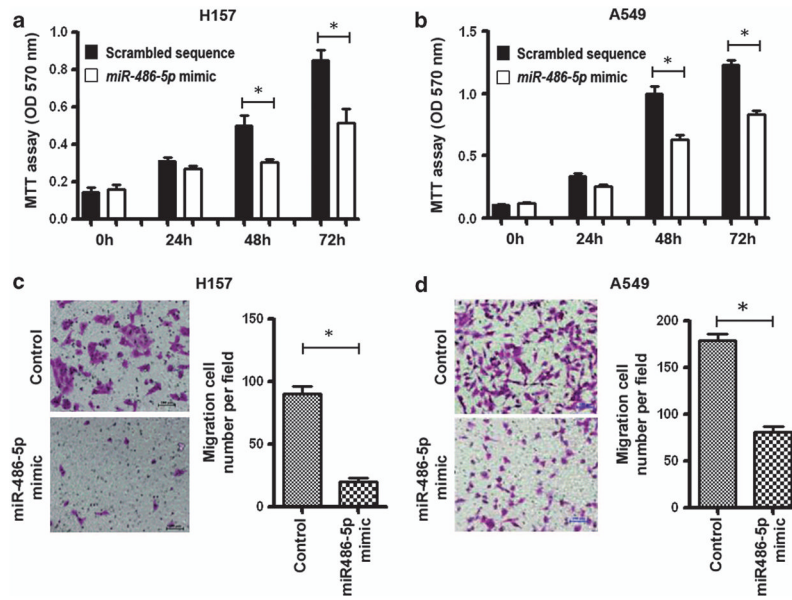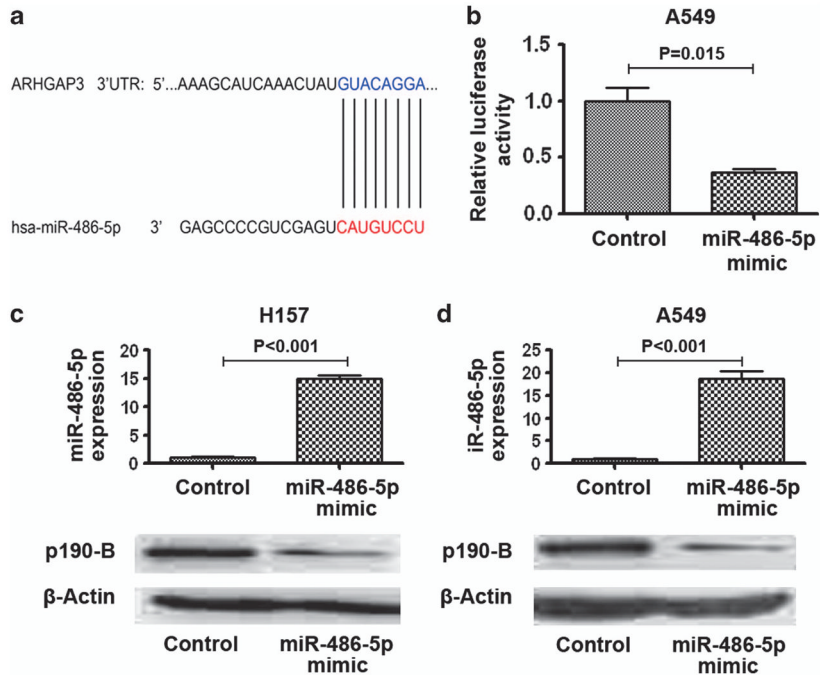
Figure 2.
MiR-486-5p suppresses NSCLC cell proliferation, migration and invasion. (**a**) Forced expression of *miR-486-5p* in H157 cells reduced cell growth determined by methylthiazol tetrazolium (MTT) assay. Cancer cells were plated in microtiter plates. On the following day, cells were transfected with *miR-486-5p* mimic or scrambled sequence, respectively. After 48 h, cell growth rate was determined by MTT. (**b**) Forced expression of *miR-486-5p* in A549 cells inhibited cell growth rate of NSCLC evaluated using MTT assay. (**c**) Ectopic expression of *miR-486-5p* in H157 cells restrained cell invasion and migration determined by Transwell assay. After transfection, cells were plated in a transwell. The cells that had migrated to the lower surface of the membrane were stained with crystal violet and counted under a light microscope. (**d**) Forced expression of *miR-486-5p* in A549 cells repressed cell invasion and migration determined by Transwell assay. All data were obtained from three independent experiments and shown as mean±s.d. and *$P<0.05$.
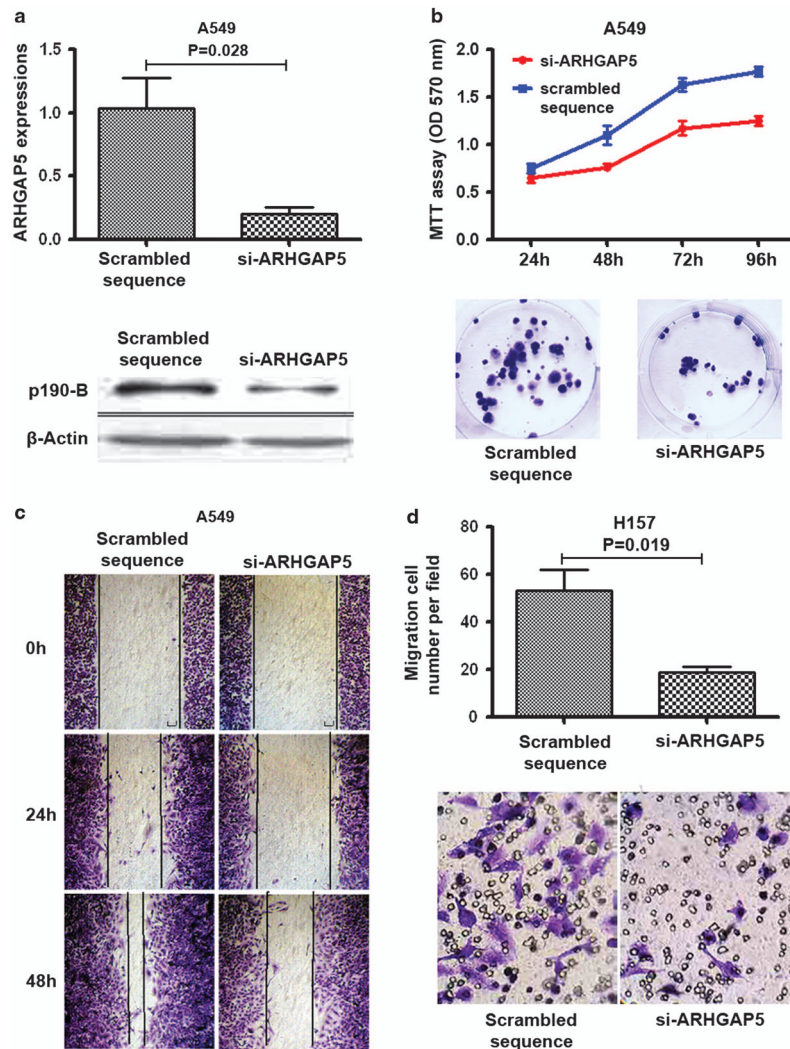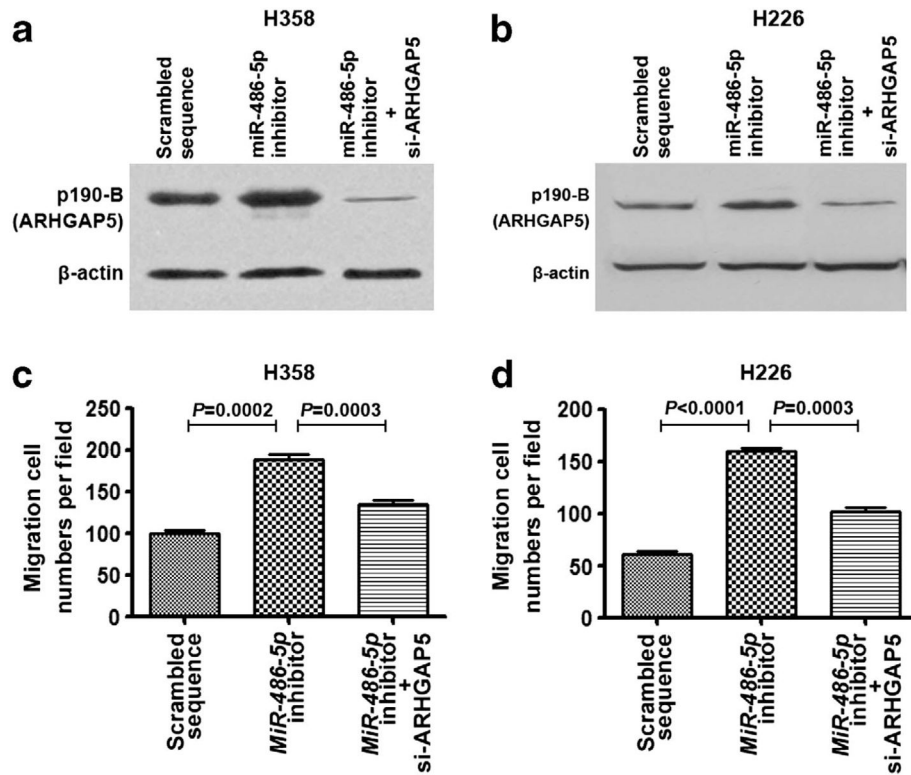
Figure 3.
Forced expression of *miR-486-5p* restrains NSCLC metastasis *in vivo*. (**a**) Fluorescent imaging analysis showed that malignant lesions in the lungs of the mice injected with H460-luc2 cells transfected with scrambled sequence after 1 week, in the neck and abdomen after 7 weeks. Ten mice were used in the group. All 10 mice were monitored by using fluorescent imaging weekly for tumor formation. The figure only shows images that were taken at week 1 and week 7 from the same mouse. (**b**) Small positive imaging signal was obtained in the lungs of the mice injected with H460-luc2 cells transfected with *miR-486-5p* mimic after 1 week, and no positive signal in the neck and lower abdomen after 7 weeks. Ten mice were used in the group and were monitored using fluorescent imaging weekly. The figure only shows images that were taken from the same mouse at week 1 and week 7. More description about the data obtained from all 10 mice from each group was shown in Supplementary Figures 4–6. (**c**) The mice were killed and autopsied in week 8 after cancer cell injection. Serial sections were made from the lungs and metastatic tumor tissues and stained with hematoxylin and eosin (H&E). H&E staining confirms that the cancer cells transfected with scrambled sequence produced tumor in the lungs. (**d**) H&E staining shows that H460 cells with scrambled sequence created a metastatic tumor in lymph node.
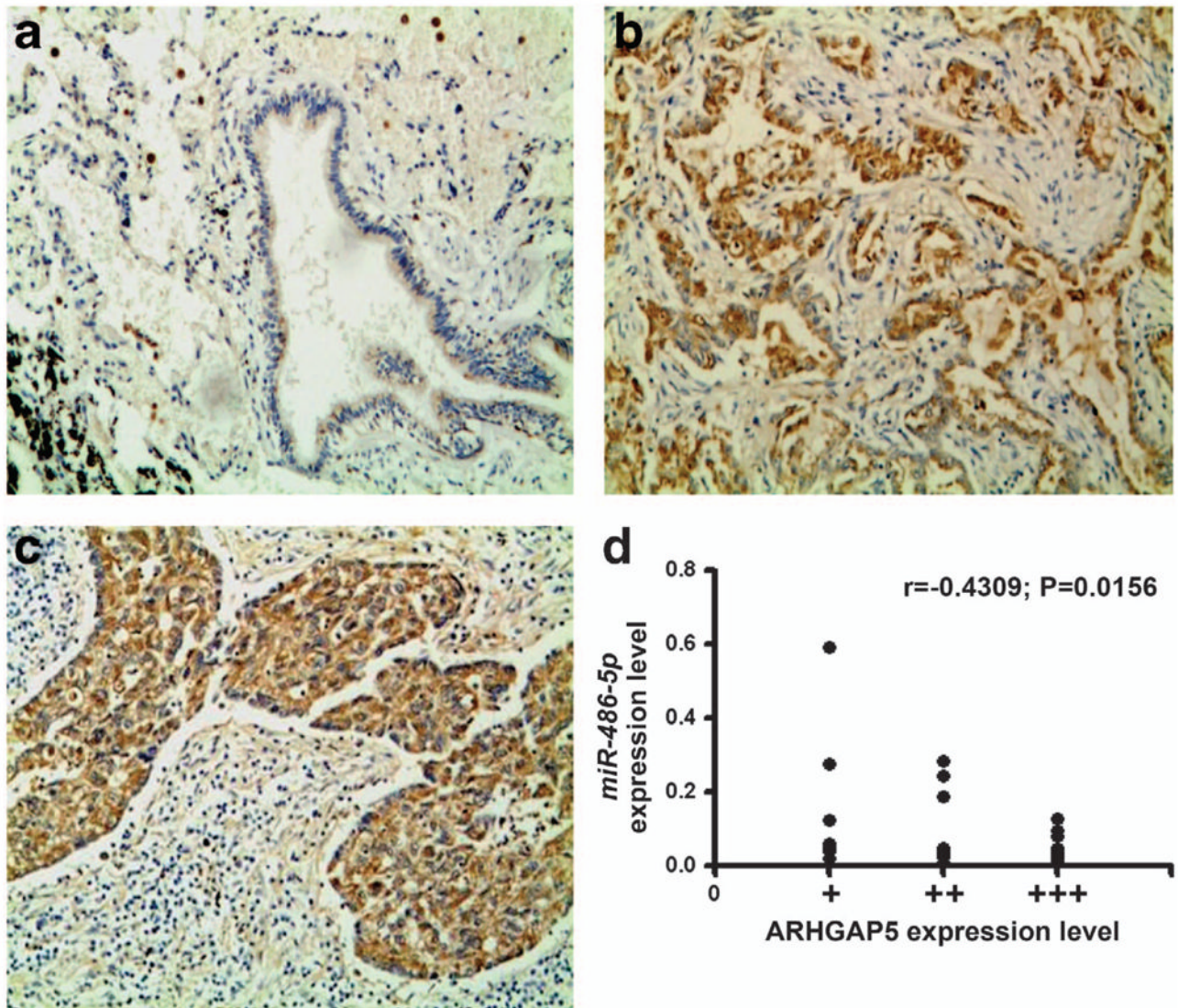
Figure 4.
ARHGAP5 is the target gene of *miR-486-5p*. (**a**) a *miR-486-5p* target site within 3′-UTR of *ARHGAP5* was predicted by bioinformatic algorithms. (**b**) A luciferase reporter assay in A549 cells showed that luciferase activity controlled by *ARHGAP5*-3′-UTR was dramatically inhibited by ectopic *miR-486-5p* expression. (**c**) Top, H157 cells had a high expression level of *miR-486-5p* after transfection with *miR-486-5p* mimic. Bottom, AHGAP5 expression level was reduced in the H157 cells transfected with *miR-486-5p* mimics determined by western blotting with p190-B antibody. (**d**) Top, A549 cells had a high expression level of *miR-486-5p* after transfection with *miR-486-5p* mimic. Bottom, the level of *ARHGAP5* protein expression was reduced in A549 cells transfected with the *miR-486-5p* mimic.

Figure 5.
Reduced expression of *ARHGAP5* inhibits cell proliferation, migration and invasion. (**a**) Top, the transcription level of *ARHGAP5* was significantly inhibited by si-*ARHGAP5* in A549 cells as determined by qRT–PCR. Bottom, *ARHGAP5* protein was repressed by the small interfering RNA at 48 h in A549 cells as determined by western blotting with p190-B antibody. (**b**) Top, methylthiazol tetrazolium assay showed that cell proliferation was decreased in A549 cancer cells transfected with si-*ARHGAP5* compared with cells with scrambled sequence. Bottom, Colony formation assay demonstrated that cell growth of A549 cells was repressed due to downregulation of *ARHGAP5*. (**c**) Wound-healing assay indicated that *ARHGAP5* downregulation inhibited cell migration and invasion of A549 cells. (**d**) Transwell assay showed that knockdown of *ARHGAP5* restrained cell migration and invasion of H157 cells.

Figure 6.
ARHGAP5 is involved in *miR-486-5p*-induced suppression of cell migration and invasion of NSCLC. (**a**) H358 cells treated with *miR-486-5p* inhibitor and si-*ARHGAP5* exhibited reduced *ARHGAP5* expression, whereas H358 cells treated with *miR-486-5p* inhibitor had increased *ARHGAP5* expression determined by western blotting with p190-B antibody. (**b**) H226 cells transfected with *miR-486-5p* inhibitor and si-*ARHGAP5* had reduced *ARHGAP5* expression, whereas H226 cells treated with *miR-486-5p* inhibitor showed elevated *ARHGAP5* expression. (**c**) H358 cells treated with *miR-486-5p* inhibitor and si-*ARHGAP5* had reduced migration and invasion potential, whereas H358 cells treated with *miR-486-5p* inhibitor displayed increased potential of migration and invasion determined by Transwell assay. (**d**) H226 cells treated with *miR-486-5p* inhibitor and si-*ARHGAP5* had reduced migration and invasion potential, whereas H226 cells treated with *miR-486-5p* inhibitor showed elevated potential of migration and invasion.

Figure 7.
ARHGAP5 is overexpressed in tumor tissues and the overexpression is inversely correlated with *miR-486-5p*. (**a**) Bronchial epithelial cells of a normal lung tissue displayed negative or weak staining of p190-B antibody. (**b**) A tissue sample of lung adeno-carcinoma showed strong immunohistochemistry staining. (**c**) A tissue sample of squamous cell carcinoma of lung had positive staining. (**d**) A scatter diagram showed an inverse correlation between *miR-486-5p* and *ARHGAP5* expressions in the same set of NSCLC tissue specimens.

Table 1

Demographic and clinical characteristics of 76 NSCLC patients and the association with *miR-486-5p* expression in tumor tissue specimens

Characteristics	Number of cases (%)	Median expression of miR-486-5p (mean±s.d.)	P
Age, year			
69	46 (60.5)	0.03182±0.03206	0.18608
<69	30 (39.5)	0.02165±0.00276	
Gender			
Male	56 (73.7)	0.03083±0.04577	0.26550
Female	20 (26.3)	0.02017±0.03556	
Histology			
Adenocarcinomas	39 (51.3)	0.02816±0.04354	0.19643
Squamous cell carcinomas	37 (48.7)	0.02253±0.02902	
Smokers[a]			
Yes	69 (90.8)	0.02126±0.03763	0.16601
No	7 (9.2)	0.03015±0.02010	
T-*status*			
1a	13 (17.1)	0.03557±0.04555	0.34540
1b	9 (11.8)	0.03106±0.02678	
2	34 (44.8)	0.03264±0.04135	
3	15 (19.7)	0.03936±0.03584	
4	5 (6.6)	0.03309±0.03276	
N-*status[b]*			
No	30 (39.5)	0.02829±0.05080	0.00190
Yes	46 (60.5)	0.01503±0.01916	
Stage			
I	19 (25.0)	0.07665±0.04979	0.00010
II	33 (43.4)	0.02830±0.01585	
III	24 (31.6)	0.01008±0.00746	

Abbreviation: NSCLC, non-small-cell lung cancer.

[a] Smokers were defined as persons who had smoked a 20 pack year, or greater.

[b] Lymph node status was classified as *N*0, *N*1, *N*2 and *N*3. In the present study, *N*1, *N*2 and *N*3 are considered to be 'Yes', whereas *N*0 is considered as 'No'.